

Slab foundation subjected to thrust faulting in dry sand: Parametric analysis and simplified design method

I. Anastasopoulos, G. Antonakos, G. Gazetas*

Laboratory of Soil Mechanics, National Technical University, Athens, Greece

ARTICLE INFO

Article history:

Received 29 May 2009

Received in revised form

25 January 2010

Accepted 3 April 2010

ABSTRACT

Motivated by recent case histories of faulting-induced damage to structures (Chi-Chi, 1999; Wenchuan 2008), this paper applies a thoroughly validated finite element analysis methodology to study the response of slab foundations subjected to thrust faulting. A parametric study is conducted, investigating the effect of key response parameters. It is shown that the stressing of the foundation, and consequently of the superstructure, stems mainly from loss of support. Depending on the geometry, loss of support takes place either *under the edges* or *under the middle* of the foundation, generating *hogging* or *sagging* deformation, respectively. Increasing the weight of the structure and/or decreasing soil stiffness leads to less stressing of the foundation. Surprisingly, even when the fault rupture emerges beyond the structure, completely avoiding the foundation, substantial foundation distress may still be generated. Exploiting the results of the parametric study, a simplified design method is developed, calling for conventional static analysis of a slab on Winkler supports, “simulating” the fault rupture by removing Winkler springs from *equivalent area(s) of loss of support*. The latter can be estimated with the help of design charts, further facilitating its use in practice. The proposed simplified method should not be viewed as a general design tool, but as a first idea of a practical solution to the investigated problem.

© 2010 Elsevier Ltd. All rights reserved.

1. Introduction

Earthquakes are typically experienced in the form of strong seismic shaking—the *indirect* result of the faulting (slip) process that emits waves into the surrounding medium. The *direct* result of the faulting process, the quasi-static fault offset, is less likely to be experienced in reality since the rupture does not always reach the ground surface. Even when it does outcrop, it will only affect structures along or near the fault trace. It is therefore understandable why earthquake engineering has mainly focused on rationally facing strong seismic shaking, while over-conservative prohibitions were the rule for protecting against fault rupture [17].

However, evidence from recent large magnitude earthquakes such as Kocaeli, Düzce-Bolu, Chi-Chi, and Wenchuan [1,10,16,18,23,25,28–31] indicates that structures may survive large fault offsets (even of the order of metres) if properly designed. Experimental and analytical studies have also confirmed that design against a “direct hit” by a rupturing fault is feasible [3–10,12,14,15,20,26].

The distress of a foundation-structure system has been shown to depend on the interplay between the upward propagating fault

rupture, the deforming soil, and the foundation-structure system. This interdependence is called “*Fault Rupture–Soil–Foundation–Structure Interaction*”, FR–SFSI [1,2]. In the absence of a structure (i.e., under free-field conditions), the rupture path and the magnitude of the surface fault scarp are functions of the fault style (normal, thrust, strike-slip), the magnitude of the fault offset at bedrock, and the nature of the overlying soil cover (thickness, soil stiffness) [9–11,13,14,20,21,27,29]. In the presence of a structure, the path of the fault rupture and the deformation of the ground surface may be substantially modified. With rigid, continuous and, especially, heavily loaded foundations, even complete diversion of the fault rupture is possible [1,5,6,15,18,19]. In addition, a heavy superstructure on soft soil will push down the foundation, thereby compressing and “flattening” the faulting-induced anomalies [5].

Recent integrated research efforts combining field studies, centrifuge experiments, and numerical analysis under the auspices of a European Research Project [4,7,8,18,19] have culminated in the development of a validated methodology for analysis of foundation–structure systems against surface fault rupture. This paper applies this methodology to study the response of slab foundations subjected to thrust (reverse) faulting. First, a parametric analysis is conducted to investigate the influence of key parameters and derive deeper insights. Then, a simplified design method is developed and validated against finite element (FE) analysis results. The proposed

* Corresponding author.

E-mail address: gazetas@ath.forthnet.gr (G. Gazetas).

simplified method should not be viewed as a general design tool, but as a first idea for a practical solution to the investigated problem. Finally, simplified non-dimensional design charts are provided for a variety of foundation–structure conditions.

2. Problem definition and analysis methodology

As depicted in Fig. 1, we consider a soil deposit of depth H subjected to thrust (reverse) faulting, which at the bedrock has a vertical component of magnitude h and a dip angle $\alpha=60^\circ$. Assuming 2D plane strain conditions, the analysis is conducted in two steps. In the first step, we analyse the propagation of the fault rupture in the free-field (i.e., in the absence of the structure). In the second step, a raft foundation of width B with surcharge load q is positioned on top of the soil model at distance s from the free-field fault outcrop (measured from the hanging-wall edge of the foundation, as shown in the figure), and the FR–SFSI analysis is conducted.

The analysis is conducted with FE modeling, which has been shown to be adequate for the simulation of fault rupture propagation through soil [11,12,3,5]. To avoid parasitic boundary effects, following the recommendation of Bray [9] the total width of the model is $B=4H$. As described in detail in Anastasopoulos et al. [2–5], we adopt an elastoplastic constitutive model with Mohr–Coulomb failure criterion and isotropic strain softening. The latter is achieved by reducing the mobilised friction ϕ_{mob} and dilation angle ψ_{mob} with increasing octahedral plastic shear strain:

$$\phi_{mob}; \psi_{mob} = \begin{cases} \phi_p - \frac{\phi_p - \phi_{res}}{\gamma_f^p} \gamma_{oct}^p; \psi_p \left(1 - \frac{\gamma_{oct}^p}{\gamma_f^p}\right), & \text{for } 0 \leq \gamma_{oct}^p < \gamma_f^p \\ \phi_{res}; \psi_{res} = 0, & \text{for } \gamma_{oct}^p \geq \gamma_f^p \end{cases} \quad (1)$$

where ϕ_p and ψ_p are the peak mobilised friction and dilation angles; ϕ_{res} and $\psi_{res}=0$ are their residual values; and γ_f^p is the octahedral plastic shear strain at the end of softening. Scale effects [22] are taken into account through an approximate simplified scaling method, described in detail in Ref. [2]. Pre-yielding behaviour is assumed to be elastic, with secant modulus $G_S = \tau_y / \gamma_y$ linearly increasing with depth. A dense sand deposit (with Young's modulus, E , varying from $E_0=5$ MPa at the ground surface to $E_H=75$ MPa at 20 m depth) is used in most of our analyses, while a

very soft silty-sand deposit (with $E_0=1$ MPa and $E_H=11$ MPa) is also used as a rather extreme example of loose/soft cohesionless soil. In all cases, the Poisson's ratio is taken equal to 0.3. The procedure utilised for model parameter calibration, based on direct shear testing, can be found in Ref. [5].

The slab foundation is modeled with elastic beam elements, connected to the soil through special contact elements. Being very stiff in compression but tensionless, such elements allow for realistic simulation of foundation detachment from the bearing soil; their response in shear obeys Coulomb's friction law, allowing for slippage at the foundation–soil interface.

The FE methodology employed herein has been extensively validated: (i) through *qualitative* and *semi-quantitative* comparisons with experimental data, as well as earlier and more recent case histories [2,3,5,13,14,18,8,28] and, most importantly, (ii) through *quantitative* genuine (Class "A") predictions of centrifuge model tests [3–5]. Fig. 2 reproduces the main results (vertical displacement Δy at the soil surface and foundation rotation $\Delta\theta$) of one such genuine prediction, referring to a rigid $B=10$ m foundation with surcharge load $q=90$ kPa, subjected to thrust $\alpha=60^\circ$ faulting through $H=15$ m Fontainebleau sand [7,8], at distance $s=9.2$ m. The comparison, although admittedly not excellent, is judged as satisfactory, especially given that some of the discrepancies are attributed to a small leakage of sand towards the glass window of the centrifuge container, spoiling somewhat the accuracy of the image analysis, as explained in Ref. [5].

3. Parametric study

A parametric analysis is conducted to derive an understanding on the interaction of a thrust–fault rupture with slab foundations. Although the analysis is undertaken for $H=20$ m, our key results and conclusions are of more general validity. According to the principles of dimensional analysis [24,22,6], and as earlier suggested by Cole and Lade [14] and Bray [9], the deformation field can be normalised with soil thickness H : i.e., the bedrock offset h and the vertical displacement Δy can be written in non-dimensional form as h/H and $\Delta y/H$. Although such normalisation is not strictly accurate (due to scale effects), it constitutes a reasonable approximation from an engineering point-of-view [2]. Accordingly, the surcharge load q and the foundation bending moment M are expressed in non-dimensional form as $q/\rho g B$ and M/qB^2 , respectively.

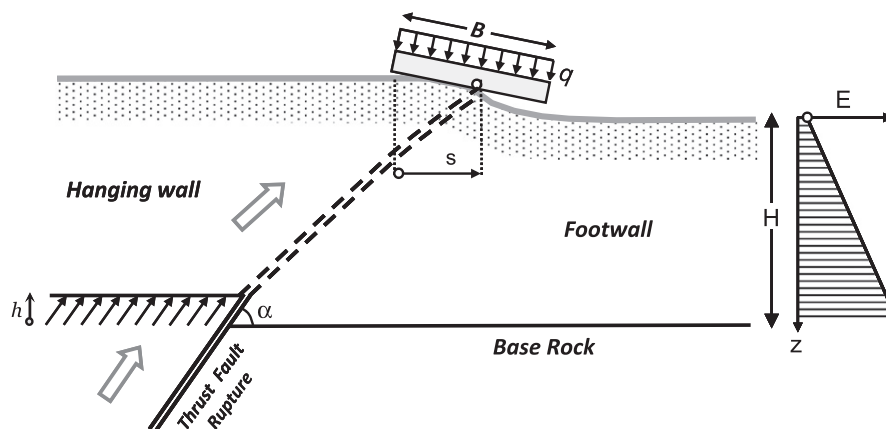


Fig. 1. Sketch of the problem and its geometry: interaction of reverse fault rupture, "propagating" upward into the soil, with a slab foundation of width B carrying a uniform load q . The left edge of the foundation is at a distance s from the point of rupture outcropping in the free field.

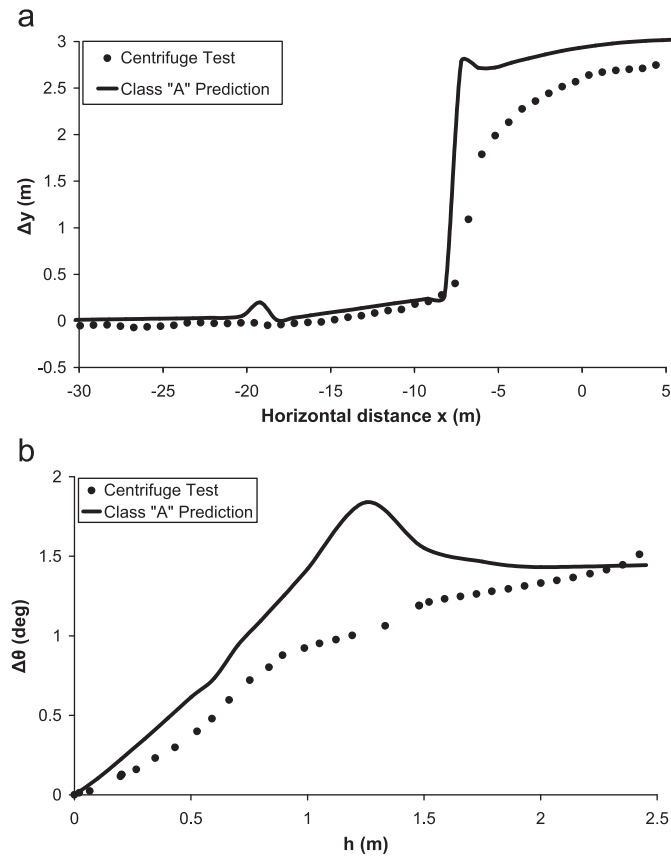


Fig. 2. Class A prediction of centrifuge model test: rigid $B=10$ m foundation with load $q=90$ kPa, subjected to thrust $\alpha=60^\circ$ faulting through $H=15$ m Fontainebleau sand deposit, positioned at distance $s=9.2$ m: (a) vertical displacement Δy at the soil surface (for $h=2.5$ m) and (b) evolution of foundation rotation $\Delta\theta$ with bedrock offset h .

The dip angle α is taken equal to 60° and the foundation slab is assumed practically rigid (i.e., very stiff; $EI=10^8$ kNm², where E is the Young's modulus of the foundation and I its moment of inertia). The following parameters are parametrically investigated:

- The location s of the structure relative to the free-field fault outcrop (measured from its hanging-wall edge): $s/B=0.1, 0.3, 0.5, 0.7, 0.9, 1.1, 1.3, 1.5,$ and 2.1 .
- The weight of the superstructure, in the form of a uniformly distributed surcharge load: $q=10, 20, 40, 60, 80,$ and 100 kPa, or in dimensionless form: $q/\rho g B=0.05, 0.1, 0.2, 0.3, 0.4,$ and 0.5 for the narrow ($B/H=0.5$) foundation, and $q/\rho g B=0.025, 0.05, 0.1, 0.15, 0.2,$ and 0.25 for the wide ($B/H=1.0$) foundation.
- The strength parameters of the soil: idealised dense sand ($\varphi_p=45^\circ, \varphi_{res}=30^\circ, \psi_p=18^\circ, \gamma_y=0.015$) and loose silty sand ($\varphi_p=32^\circ, \varphi_{res}=30^\circ, \psi_p=3^\circ, \gamma_y=0.030$). The depth-dependent values of the Young's modulus in the two soils were given previously.

In the following sections, only the key results of the parametric analysis are presented and discussed.

3.1. The effect of fault rupture location

To highlight the effect of the location s/B of the outcropping fault rupture relative to the hanging-wall side (left edge) of the structure, we focus on the response of a $B/H=0.5$ (i.e., $B=10$ m) foundation subjected to surcharge load $q/\rho g B=0.1$

(i.e., $q=20$ kPa), positioned at $s/B=0.1, 0.5, 0.9, 1.1, 1.5,$ and 2.1 . The comparison for the first three locations (corresponding to the fault rupture emerging within the limits of the foundation) is shown in Fig. 3 in terms of:

- deformed mesh with superimposed plastic shear strain contours (for bedrock offset $h/H=10\%$);
- evolution with increasing base dislocation (h/H from 0% to 10%) of the dimensionless contact pressures p/q ;
- normalised foundation bending moments M/qB^2 .

The following trends are worth to be noted:

First, observe in all cases the “refraction” of the rupture plane as it “enters” from the rock into the soil and propagates towards the ground surface. Moreover, as depicted in Fig. 3a, for $s/B=0.1$ (i.e., $s=1$ m) the rupture is clearly diverted towards the hanging wall, i.e. to the right of the foundation. But, despite this beneficial diversion, the foundation experiences significant stressing. Initially, before the event of the earthquake, i.e. for $h/H=0$, the foundation is in full contact with the bearing soil: p/q is slightly less than 1 (in absolute terms) over most of the foundation width, i.e. for about $0.1 < x/b < 0.9$, slightly increasing (in almost linear fashion) to about 1.5 at the edges. The reader may recall that our particular inhomogeneous soil profile lies between the homogeneous soil (for which the elasticity solution predicts edge stresses that tend to infinity – singular points) and the ‘Gibson’ incompressible ($\nu=0.50$) soil of Young's modulus, E , proportional to depth (for which the solution is a uniform pressure distribution – a perfect Winkler medium).

For $h/H=1.5\%$, although the rupture has not yet outcropped, some changes in the distribution of p/q start being noticeable. The resulting M/qB^2 is almost two times larger than its initial pre-seismic value M_o . Increasing the bedrock offset to $h/H=3.5\%$, the rupture outcrops at the hanging-wall edge of the foundation, creating loss of contact at its centre (for $0.4 < x/b < 0.8$); i.e., it is now supported only on its two edges: $x/b \leq 0.4$ and $x/b \geq 0.8$. This effectively renders the foundation a single span beam on “elastic” end supports. As a result, the raft develops a bending moment almost five times larger than M_o . Further increasing h/H to 5% and 10% does not seem to have an appreciable effect: soil reactions, p , and developing bending moments, M , remain practically unchanged for all values of h/H exceeding 3.5%.

When the fault rupture emerges under the middle of the foundation (i.e., $s/B=0.5$), the response becomes substantially different. As illustrated in Fig. 3b, the rupture now cannot be diverted and the plastic deformation is more diffused under the foundation. For $h/H=1.5\%$, the distribution of soil pressures becomes less uniform than before the event, with larger (compressive) stresses under the edges. As a consequence, M becomes almost three times larger than M_o . Then, for $h/H=3.5\%$, the rupture outcrops beneath the foundation, thereby causing loss of support: below the left edge, from $x/b=0-0.15$; and below the middle to the right, from $x/b=0.6-0.9$, as evidenced from the vanishing soil pressures p . The unsupported left span essentially acts as a cantilever on “elastic” supports, while the one at the middle-right as a “simply” supported beam. The outcome of this rather dramatic change in the support conditions is a reversal of the stressing, with M/qB^2 changing sign to reach -0.02 (or M becomes roughly equal to $-M_o$): i.e., the slab experiences “hogging” instead of “sagging” deformation. Interestingly, for a much larger dislocation, $h/H=10\%$, the foundation regains contact at its left edge, practically cancelling the cantilever-type left span and reducing the “hogging” moment to $M/qB^2=-0.01$. Since the cantilever at the left was counter-balancing the middle-right

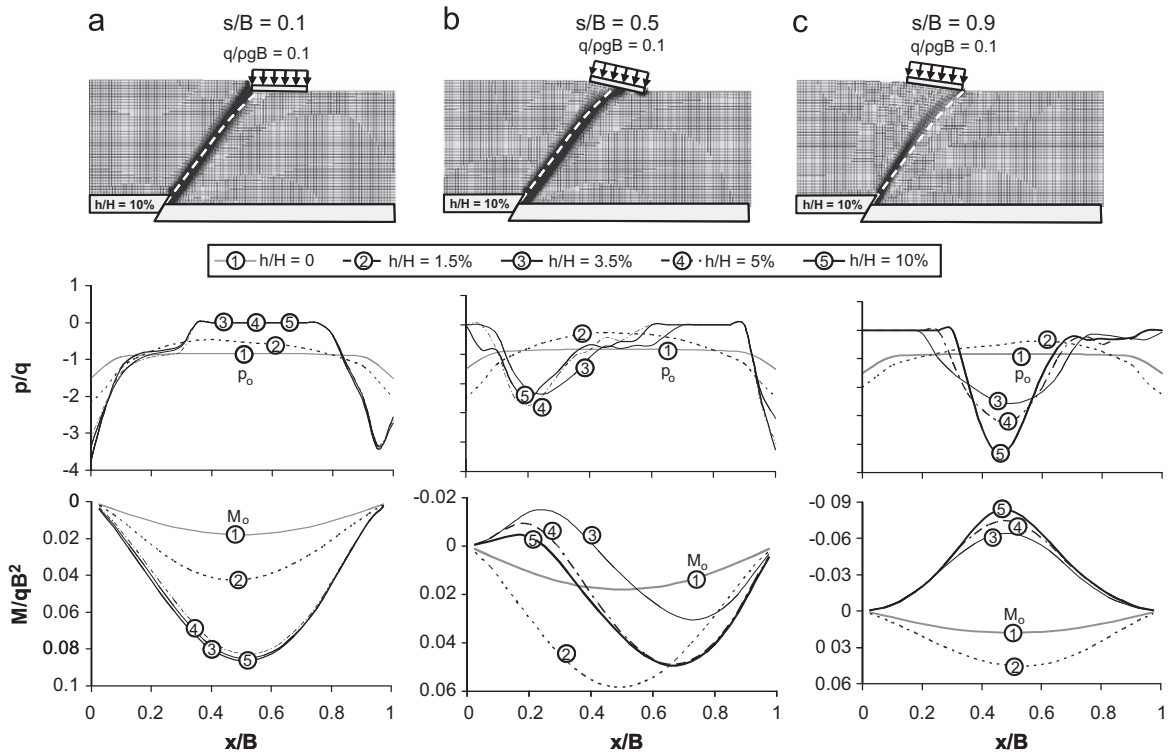


Fig. 3. The effect of fault rupture location s : the “direct-hit” cases. (a) $s/B=0.1$, (b) $s/B=0.5$, and (c) $s/B=0.9$. From top to bottom: deformed mesh with zone of large plastic strain, for $h/H=10\%$ (top row); normalised contact pressures p/q (middle row); and normalised foundation bending moment M/qB^2 (bottom row). Narrow $B/H=0.5$ foundation, with surcharge load $q/\rho g B=0.1$. The dotted white line represents the rupture plane in the unperturbed free field.

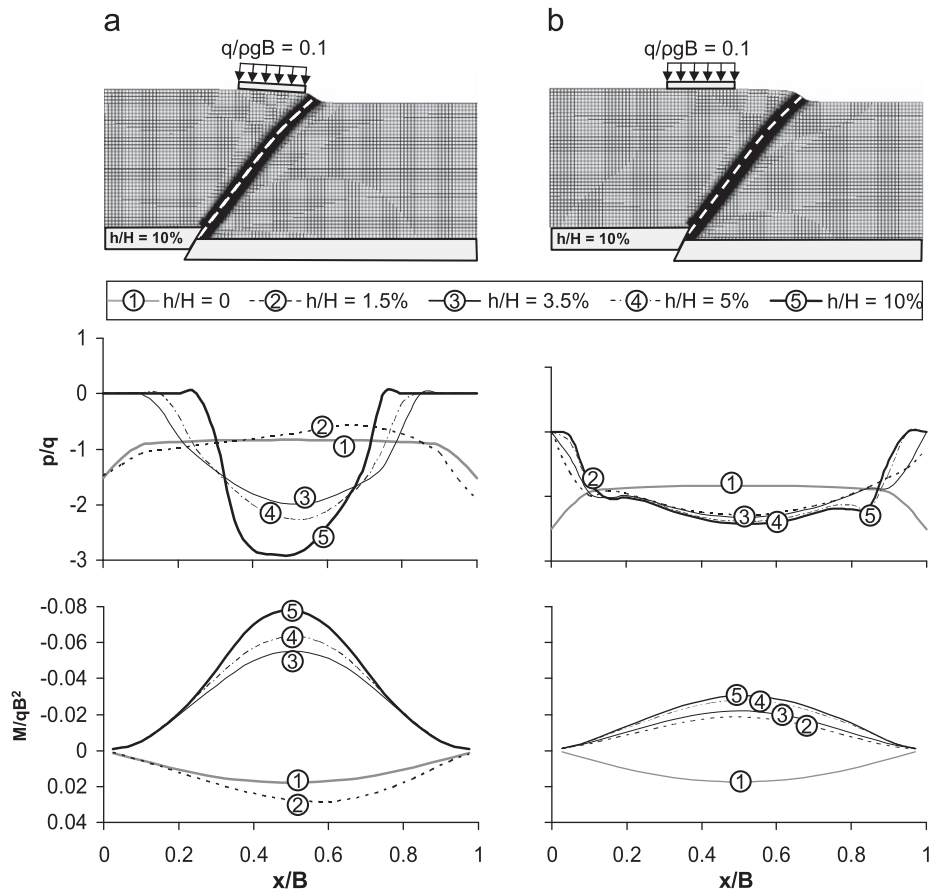


Fig. 4. The effect of fault rupture location s : the “indirect hit” cases. (a) $s/B=1.1$ and (c) $s/B=2.1$. From top to bottom: deformed mesh with zone of large plastic strain, for $h/H=10\%$ (top row); normalised contact pressures p/q (middle row); and normalised foundation bending moment M/qB^2 (bottom row). Narrow $B/H=0.5$ foundation, with surcharge load $q/\rho g B=0.1$.

simply supported-type span, the “sagging” bending moment now increases (in absolute terms) substantially, to almost $-2.5M_o$.

Moving the rupture close to the footwall-side (right edge) of the foundation ($s/B=0.9$) simplifies the picture: initially, for $h/H=1.5\%$, although the changes in p from the static pressure distribution are not very pronounced, M is almost doubled ($\approx 2M_o$). Then, for $h/H=3.5\%$, the rupture outcrops under the right edge of the foundation, and leads to loss of support under both edges. The resulting, two cantilevers cause a reversal of the stressing (“hogging” instead of “sagging” deformation), with M/qB^2 reaching -0.08 (i.e., roughly $-4M_o$). Further increasing of h/H does not lead to any remarkable change.

Since in many thrust-fault earthquakes (e.g., Chi-Chi, 1999) serious structural damage has also been reported not directly on the fault but on the hanging-wall segment, at some distance from the fault scarp, we also investigate in Fig. 4 two cases in which the fault rupture outcrops outside the width of the structure: $s/B=1.1$ and 2.1 . For $s/B=1.1$ (Fig. 4a), the rupture outcrops close to the footwall-side (right edge) of the foundation and the whole response is very similar to the $s/B=0.9$ case. For $h/H=1.5\%$, p is barely altered at all and M only slightly exceeds M_o . Then, for $h/H=3.5\%$, with the rupture outcropping close to the foundation, loss of support is noticed at the two edges. The width of the two unsupported (cantilevered) spans increases with increasing bedrock offset, until for $h/H=10\%$ it reaches about 1/3 of the foundation width (on each side), while only the middle 1/3 of the foundation carries all vertical load. As a consequence, the stressing is completely reversed and M is almost as large as in the “direct-hit” case of $s/B=0.9$ case (Fig. 3).

With the fault rupture emerging further away (to the right) a decrease of the unsupported spans and thereby of the foundation distress is hardly surprising. But even for $s/B=2.1$ (Fig. 4b), although the extent of loss of support is quite limited (to about 5% of the foundation width on each side), the distress of the foundation is non-negligible ($M \approx -1.5M_o$). Most importantly, the foundation is still subjected to “hogging” deformation, which is exactly the opposite of what it would have been statically designed for (i.e., “sagging”). Hence, even if the rupture does not cross the structure (in this particular case, it missed the foundation by 12 m), structural damage is quite likely without proper design, as reinforcement would have been placed in the opposite side.

Fig. 5 summarizes the effect of s/B for the same foundation–structure system on: (a) the normalised vertical displacement $\Delta y/H$ at the soil surface (for the largest considered dislocation: $h/H=10\%$); (b) foundation rotation $\Delta\theta$ with respect to bedrock offset h/H for five specific values of s/B ; and (c) normalised bending moment M/qB^2 for $h/H=10\%$ and the same s/B values. Notice that when the rupture outcrops to the left of the foundation centerline (i.e., for $s/B \leq 0.5$), loss of support takes place near its centre (Fig. 5a). In marked contrast, when the rupture outcrops to the right of its centerline (i.e., for $s/B > 0.5$), it is the two edges that experience loss of support.

The maximum $\Delta\theta$ ($\approx 10^\circ$ for $h/H=10\%$) is attained for $s/B \approx 0.5$ (Fig. 5b). In case of a “direct hit”, i.e. when the rupture emerges directly underneath the foundation (i.e., $0 \leq s/B \leq 1.0$), $\Delta\theta$ increases with increasing dislocation ratio h/H . In stark contrast, when emerging outside its borders (i.e., $s/B > 1.0$ —“indirect hit”), $\Delta\theta$ is a nonlinear function of dislocation, reaching nearly constant “ultimate” values for $h/H \geq 2\%$. For $s/B \geq 1.5$, $\Delta\theta$ is about 1° , and for $s/B=2.1$ about 0.5° . This highly nonlinear behaviour stems from the fact that the fault rupture is not crossing the foundation; hence, once the rupture has outcropped ($h/H > 2\%$), most of the imposed deformation is localised along the rupture zone, with no more quasi-elastic bending deformation of the hanging wall. A qualitatively similar phenomenon has been observed with

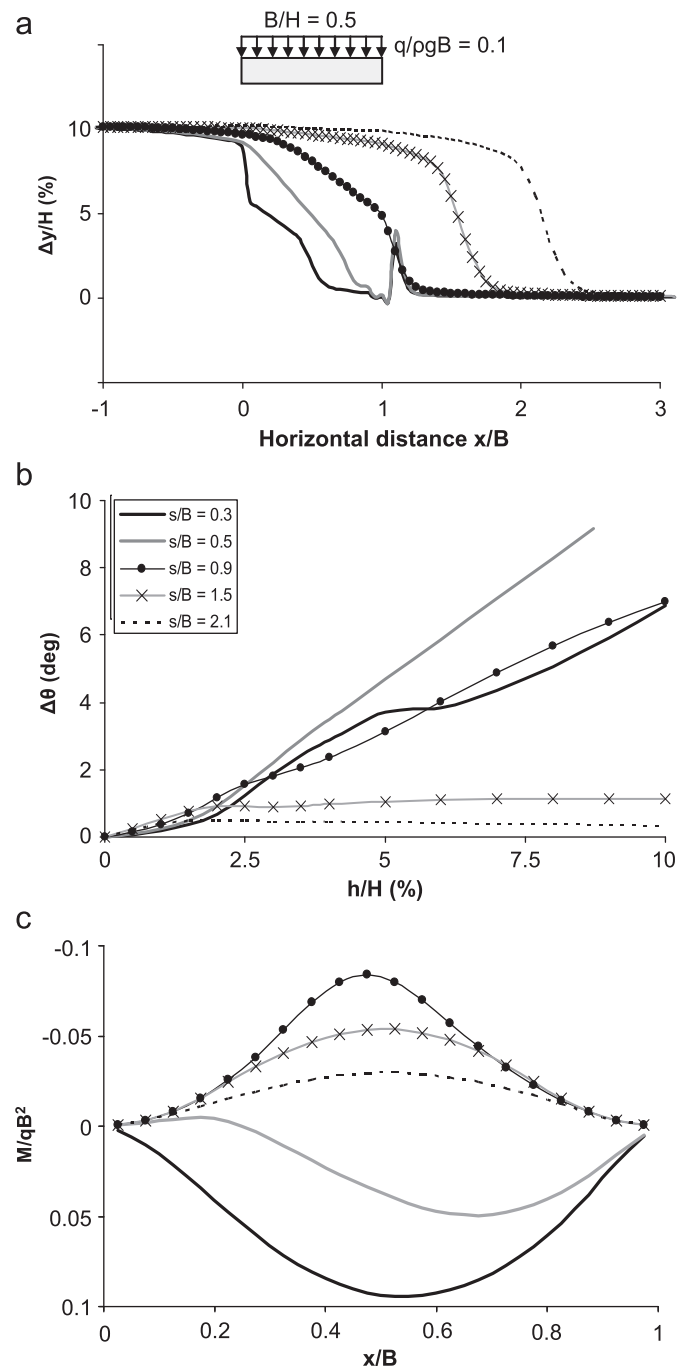


Fig. 5. The effect of fault rupture location s/B ; narrow $B/H=0.5$ foundation with surcharge load $q/\rho g B=0.1$: (a) normalised vertical displacement $\Delta y/H$ along the ground surface (for $h/H=10\%$); (b) foundation rotation $\Delta\theta$ with respect to bedrock fault offset h/H ; and (c) normalised bending moment M/qB^2 (for $h/H=10\%$).

normal faulting [4,19]. Since the stressing of the foundation arises only from such bending deformation, it attains a “stable” condition after some loss of support from its two edges, “enjoying” the continued upward “ride”, i.e. without suffering any further distress with the movement of the hanging wall. In contrast, when the rupture crosses the foundation (i.e., $s/B < 1.0$), the increase of h/H is associated with redistributions and mechanism changes, leading to an essentially linear increase of $\Delta\theta$ with h/H .

As summarised in Fig. 5c, moving the rupture from the left side to the right side of the foundation, the faulting-induced bending moments reverse sign: for $s/B \leq 0.5$ (i.e., to the left of the

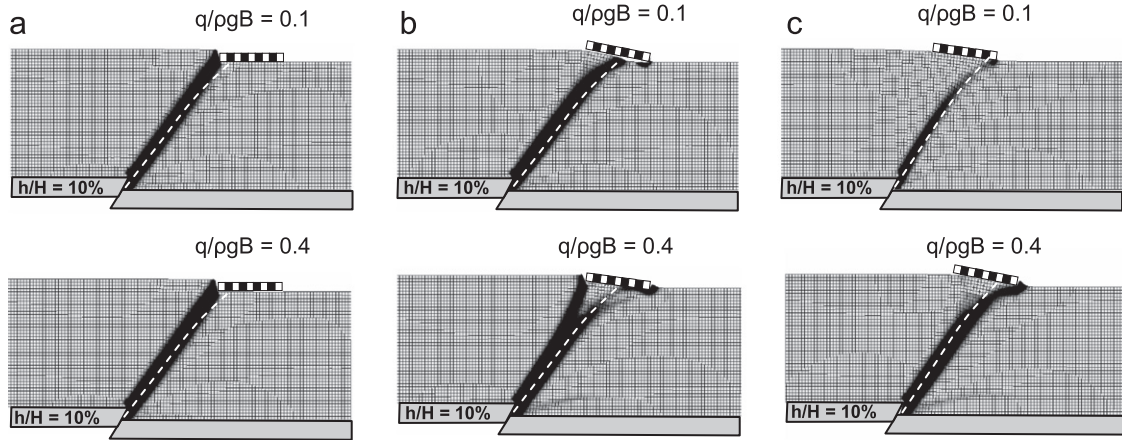


Fig. 6. The effect of superstructure weight, expressed through the load $q/\rho g B$; narrow $B/H=0.5$ foundation: (a) $s/B=0.1$; (b) $s/B=0.5$ and (c) $s/B=0.9$. From top to bottom, deformed mesh with shear strain contours for $q/\rho g B=0.1$ and 0.4 .

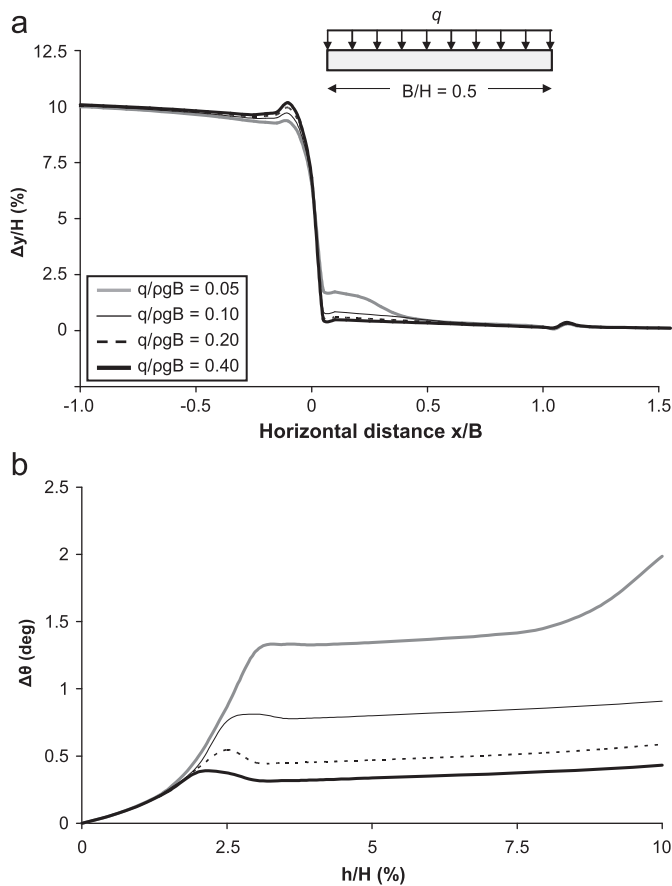


Fig. 7. The effect of superstructure weight, expressed through the surcharge load $q/\rho g B$, on: (a) normalised vertical displacement $\Delta y/H$ at the soil surface (for $h/H=10\%$) and (b) foundation rotation $\Delta\theta$ with respect to bedrock offset h/H (narrow $B/H=0.5$ foundation subjected to thrust faulting at $s/B=0.1$).

centerline) the foundation is subjected to *sagging* deformation; for all other cases ($s/B > 0.5$, i.e., to the right of the centerline), *hogging* deformation prevails.

3.2. The effect of the superstructure weight

To focus on the effect of superstructure weight, we compare the response of the same $B/H=0.5$ foundation subjected to

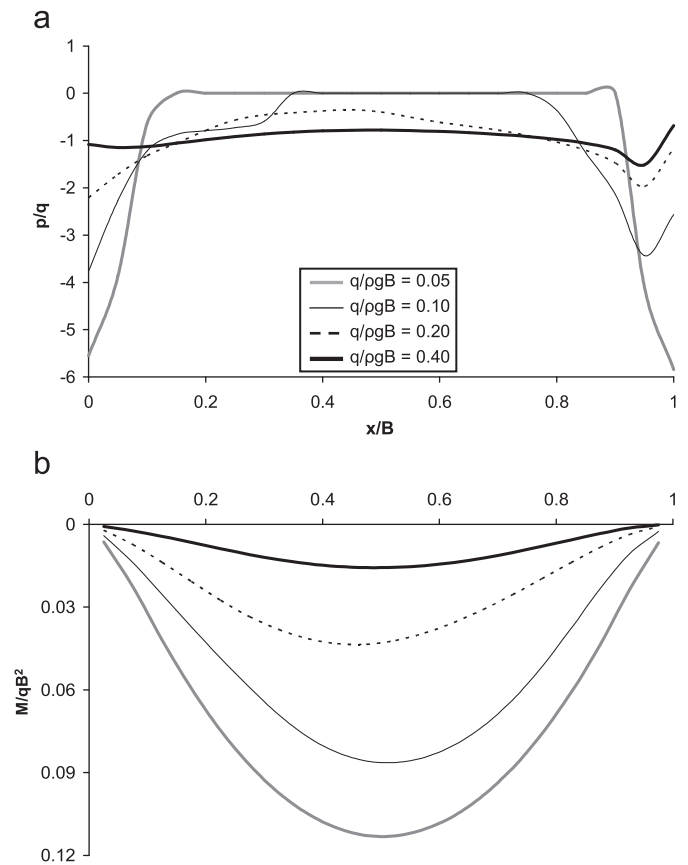


Fig. 8. The effect of superstructure weight, expressed through the surcharge load $q/\rho g B$, on: (a) normalised contact pressure p/q and (b) normalised bending moment M/qB^2 . ($h/H=10\%$, narrow $B/H=0.5$ foundation, thrust faulting emerging at $s/B=0.1$ in the free field.)

surcharge load $q/\rho g B=0.1$ and 0.4 (or $q=20$ and 80 kPa), positioned at $s/B=0.1, 0.5$, and 0.9 .

Fig. 6 summarizes the comparison in terms of deformed mesh with superimposed plastic shear strains for $h/H=10\%$. For $s/B=0.1$ the effect of the superstructure weight on the ground settlement profile Δy and the foundation rotation $\Delta\theta$ is shown in Fig. 7, while the effect on the soil reactions p and bending moments M in Fig. 8. For the other extreme case of $s/B=0.9$ (rupture outcrops close to the right edge of the foundation), Figs. 9 and 10 show respectively

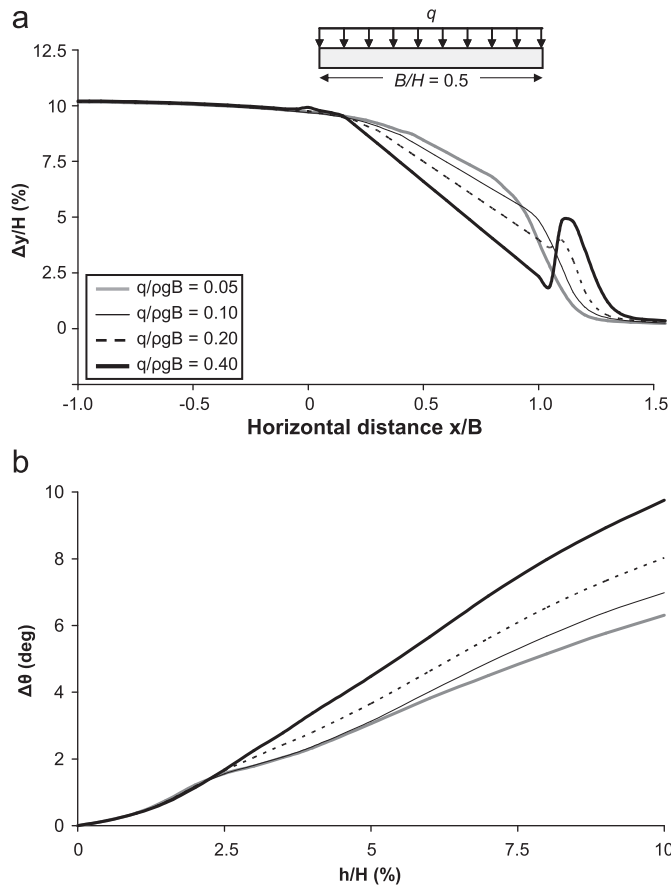


Fig. 9. The effect of superstructure weight, expressed through the surcharge load $q/\rho g B$, on: (a) the normalised vertical displacement $\Delta y/H$ at the soil surface (for $h/H=10\%$) and (b) the foundation rotation $\Delta \theta$ with respect to bedrock offset h/H . (Narrow $B/H=0.5$ foundation, thrust faulting emerging at $s/B=0.9$ in the free field.)

($\Delta y/H$, θ) and ($q/\rho g B$, M/qB^2). The following conclusions emerge from these figures:

- For $s/B=0.1$, the increase in superstructure weight (or the mean applied pressure) has a dramatically beneficial effect. While the foundations of light structures (i.e., $q/\rho g B=0.05$ and 0.10) are largely detached from the supporting soil at the centre (for about 80% and 40% of their width, respectively), heavier structures ($q/\rho g B=0.20$ and 0.40) retain full contact—as clearly evidenced from the soil pressures (vanishing only in the former two cases). A direct consequence is that the normalised bending moments M/qB^2 decrease by a factor of almost 5 with the heavier structure. At the same time, $\Delta \theta$ is also significantly reduced (Fig. 7b): from 2° for $q/\rho g B=0.05$ to merely 0.4° for $q/\rho g B=0.4$. Also notice that while $\Delta \theta$ increases almost linearly with h/H for small bedrock offsets ($h \leq 2.5\%$), it is hardly affected by further increase of h/H for all loading cases.
- For $s/B=0.9$, the increase in superstructure weight is again beneficial, although to a lesser degree than for $s/B=0.1$. Detachment of the foundation from the supporting soil ($p=0$) takes place in all cases, but for the heavier loaded foundation ($q/\rho g B=0.4$) this is limited to only 10% of footing width under the left edge of the foundation. The resulting normalised bending moment, M/qB^2 , is now smaller by a factor of 2.5 compared to the moment of the lightest foundations ($q/\rho g B=0.05$). But in contrast to the $s/B=0.1$ case, it is now the heavier foundation that experiences the largest rotation ($\Delta \theta \approx 10^\circ$ vs. $\Delta \theta \approx 6^\circ$, for $h/H=0.1$). Moreover, in stark

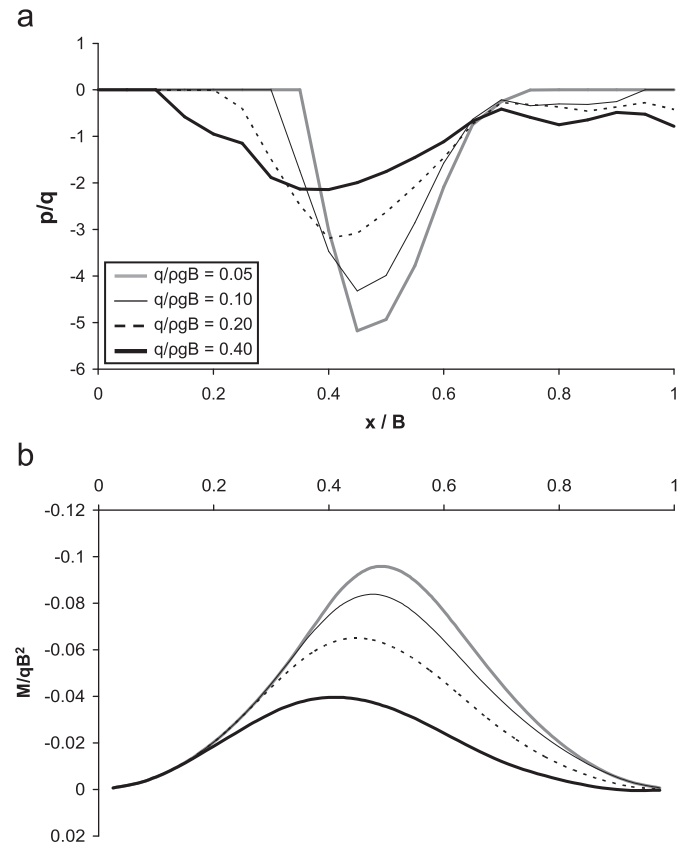


Fig. 10. The effect of superstructure weight, expressed through the surcharge load $q/\rho g B$, on: (a) the normalised contact pressure p/q and (b) the normalised bending moment M/qB^2 . ($h/H=10\%$, narrow $B/H=0.5$ foundation, thrust faulting emerging at $s/B=0.9$ in the free field.)

contrast to the $s/B=0.1$ case, due to mechanism changes and stress redistributions, $\Delta \theta$ now increases monotonically with q (almost in linear fashion).

- When the rupture emerges under the middle of the foundation, $s/B=0.5$, the interaction becomes a little more complicated (Fig. 6b). While the lightest considered superstructure hardly affects the rupture path, heavier structures lead to diffusion of plastic deformation, and some diversion towards the footwall (to the right); with the heaviest considered structure ($q/\rho g B=0.4$) bifurcation takes place, with the main rupture being diverted to the hanging-wall edge of the foundation. As a result $\Delta \theta$ is reduced appreciably.

3.3. The effect of soil stiffness and strength

To illustrate the effect of soil stiffness, we compare the response of the $B/H=0.5$ foundation with $q/\rho g B=0.1$ (i.e., $q=20$ kPa) supported on two idealised soil profiles: a dense sand and a very loose silty-sand deposit. Due to space limitations, we only show the results for $s/B=0.1$ (i.e., fault rupture outcropping near the hanging wall, left, edge of the foundation). The key conclusions are similar for other fault rupture outcropping locations.

Although the differences between the two soils in the $\Delta y/H$ profile are not readily discernible (Figs. 11a and b), they nevertheless become conspicuous in terms of p/q (Fig. 11c) and M/qB^2 (Fig. 11d). While on dense sand the foundation experiences rather pronounced loss of contact under its middle

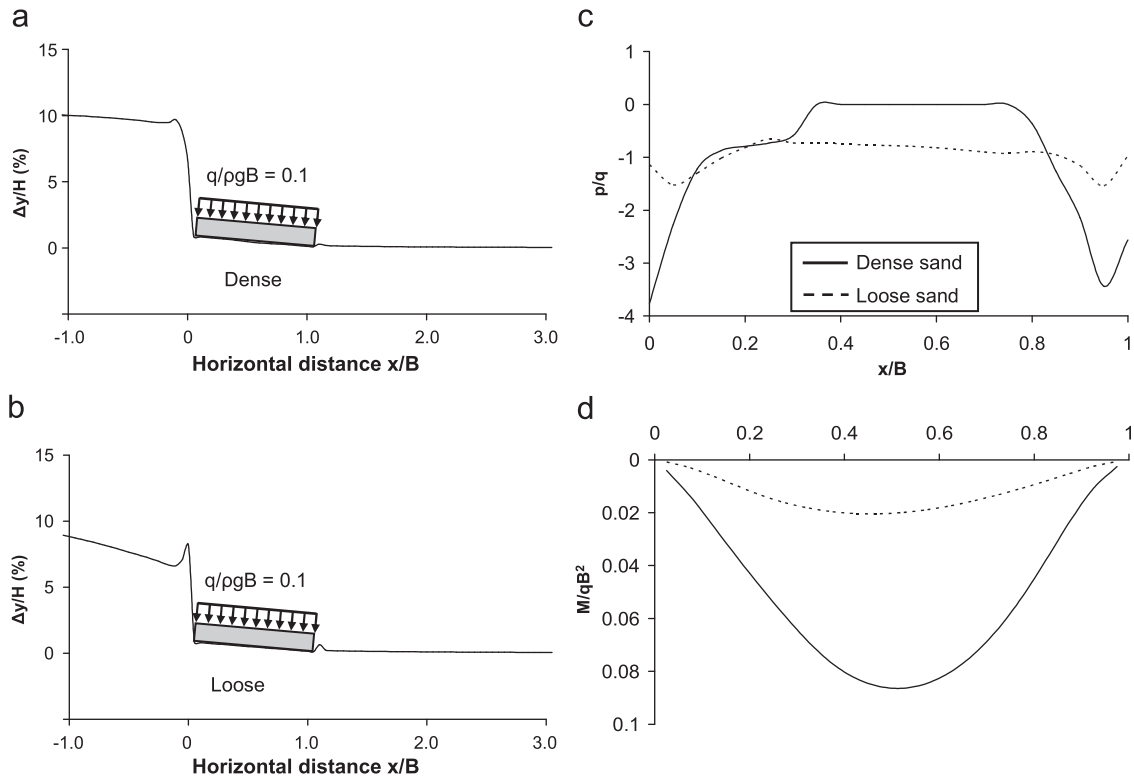


Fig. 11. The effect of soil compliance: (a) normalised vertical displacement $\Delta y/H$ of the ground surface for dense soil and (b) $\Delta y/H$ for loose soil; (c) normalised contact pressures p/q and (d) normalised bending moment M/qB^2 . (Narrow $B/H=0.5$ foundation, surcharge load $q/\rho g B=0.1$, thrust faulting emerging at $s/B=0.1$, $h/H=10\%$.)

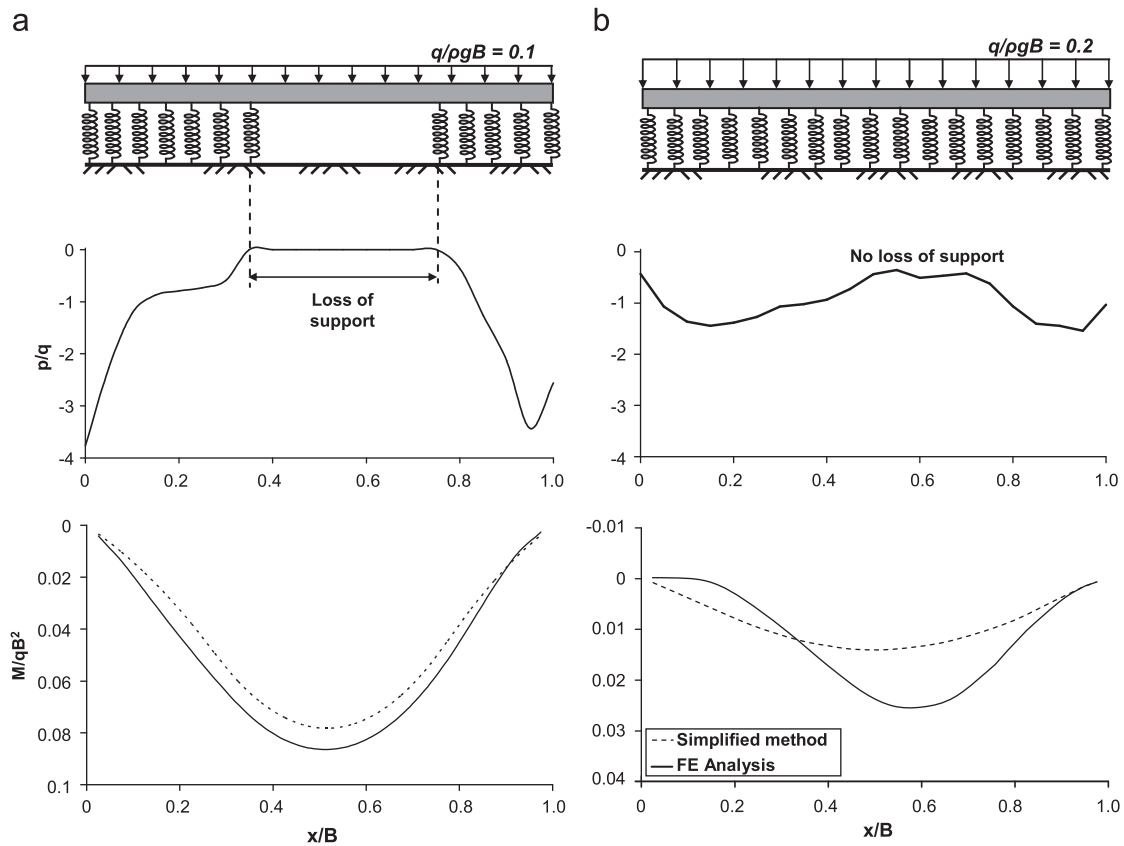


Fig. 12. Example comparison of the simplified method (removal of Winkler springs under the area of loss of support) with FE analysis results, in terms of M/qB^2 : (a) $B/H=0.5$ foundation with $q/\rho g B=0.1$ subjected to faulting at $s/B=0.1$ through dense sand and (b) $B/H=0.5$ foundation with $q/\rho g B=0.2$ subjected to faulting at $s/B=0.7$ through loose silty sand. While in the first case (in which soil detachment prevails) the comparison is quite acceptable, in the latter case (in which no complete loss of support is observed) the simplified method underestimates the distress of the foundation by a (significant) factor of nearly 2.

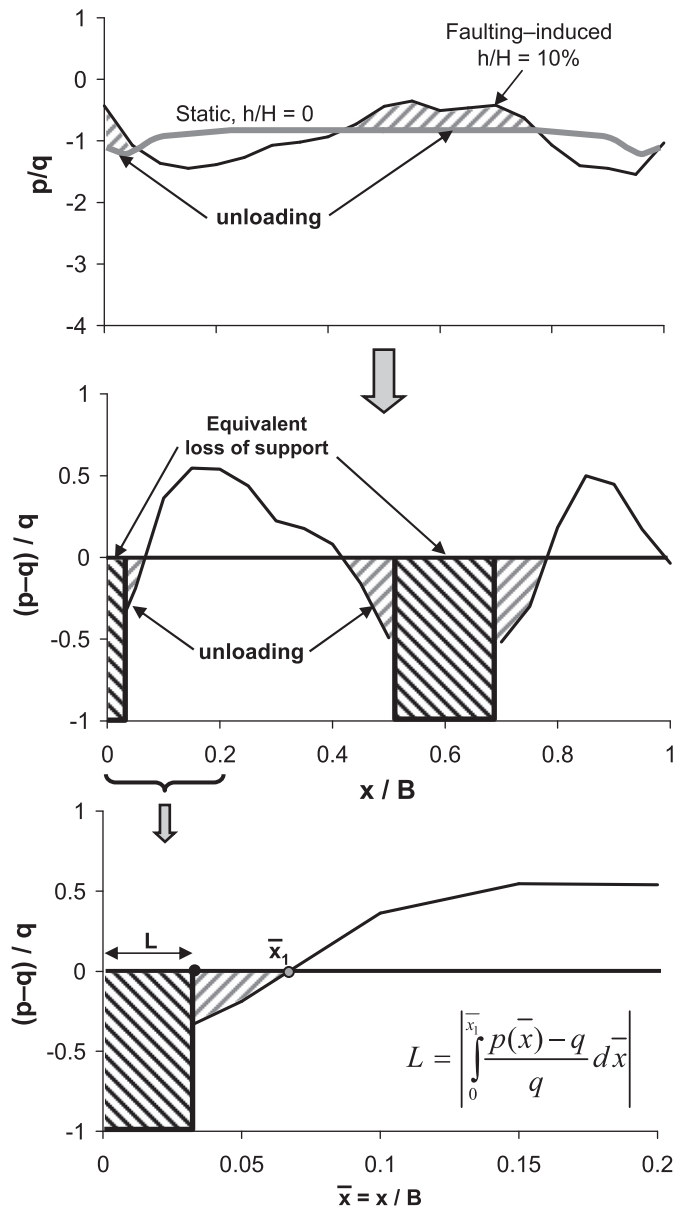


Fig. 13. Sketch illustrating the main concept of the improved simplified method.

($0.35 < x/B < 0.75$), on the very loose soil contact is maintained throughout its whole width. As a result, the faulting-induced stressing decreases substantially with increasing soil compliance: the maximum M is reduced from $4M_0$ in dense sand to almost M_0 (i.e., there is almost no additional distress due to faulting).

4. Simplified design method

4.1. The main concept

As already discussed, depending on the location of the outcropping fault rupture relative to the structure, detachment may take place either at the middle or at the two edges of the foundation. In the first case, the unsupported span will behave as a simply supported beam on elastic supports, imposing “sagging” deformation onto the foundation–structure system; in the latter case, the unsupported end spans will act as cantilevers on a central elastic support, producing “hogging” deformation. Since the stressing of the foundation is directly related to this loss of

support, the results of our analysis can be utilised directly for the design of a foundation–structure system against faulting, just by removing the Winkler-type springs (i.e., the supports typically used in structural design software) from the area(s) of loss of support due to soil detachment.

An example of this simplified design procedure is outlined in Fig. 12. We compare the stressing of the foundation in terms of M/qB^2 as computed with FE analysis, to the simplified procedure of Winkler spring removal from the area of loss of support. The figure refers to a narrow $B/H=0.5$ foundation with $q/\rho gB=0.1$ subjected to faulting at $s/B=0.1$ on dense sand (Fig. 12a), and for the same foundation but with a heavier superstructure $q/\rho gB=0.2$ subjected to faulting at $s/B=0.7$ on loose sand (Fig. 12b). While in the first case (in which soil detachment is prevailing), the comparison is quite acceptable, in the latter case (in which no detachment is observed) the simplified method grossly underestimates the distress of the foundation. The cause is rather obvious: a substantial decrease in soil reactions may be enough to produce a considerable increase of bending moments even if no uplifting takes place.

Hence, to render the simplified design method applicable to all cases, it is necessary to slightly modify its main concept. For this purpose, we define area(s) of equivalent “loss” of support, as schematically illustrated in Fig. 13. The p/q diagram (top) compares the faulting-induced foundation contact pressures (black thin line) to the static ones ($h/H=0$, grey thick line). The grey-shaded areas correspond to the areas of the foundation where p/q is reduced due to the imposed tectonic deformation. Notice that this reduction does not lead to any soil detachment ($p \neq 0$). A clearer picture can be drawn through the $(p-q)/q$ diagram (middle): partial reduction of soil support takes place when $(p-q)/q$ is negative (see grey-shaded areas). If detachment had taken place, $(p-q)/q$ would equal -1 . The same happens if we remove the spring supports, which is the key objective of the simplified method. The equivalent area(s) of loss of support are black-shaded in the figure. We explain their logic through the bottom diagram, which focuses on the first (from the left) such area. The area where partial reduction of soil support is observed spans from $x/B \equiv \bar{x}=0$ to \bar{x}_1 (grey shaded). Assuming approximate equivalence in terms of area, we define the length L of the area of equivalent loss of support (black-shaded) as follows:

$$L = \left| \int_0^{\bar{x}_1} \frac{p(\bar{x})-q}{q} d\bar{x} \right| \tag{2}$$

Since the distribution of $(p-q)/q$ is responsible for the development of M/qB^2 , by removing the spring supports from this area (of length L), we can achieve a roughly similar stressing. Admittedly, it will not be argued that this can offer anything more than a crude approximation.

4.2. Illustration of the effectiveness of the simplified method

The above procedure was applied to all of the investigated cases. Using the distribution of $(p-q)/q$ as computed through FE analysis, we estimate for each case the equivalent area(s) of loss of support (i.e., the equivalent lengths L). Then, we conduct a simplified beam-on-Winkler spring analysis, removing the spring supports from these areas of “effective” detachment. The whole procedure was applied for bedrock offset $h/H=5\%$ and 10% . Fig. 14 compares the simplified method with FE analysis results in terms of M/qB^2 , for the case of dense sand. The comparison is shown for $h/H=10\%$, for both the narrow $B/H=0.5$ and the wide $B/H=1.0$ foundation subjected to a variety of superstructure loads q , and for $s/B=0.1, 0.5$, and 0.9 . With only few exceptions, the simplified procedure is in satisfactory agreement with the more rigorous FE

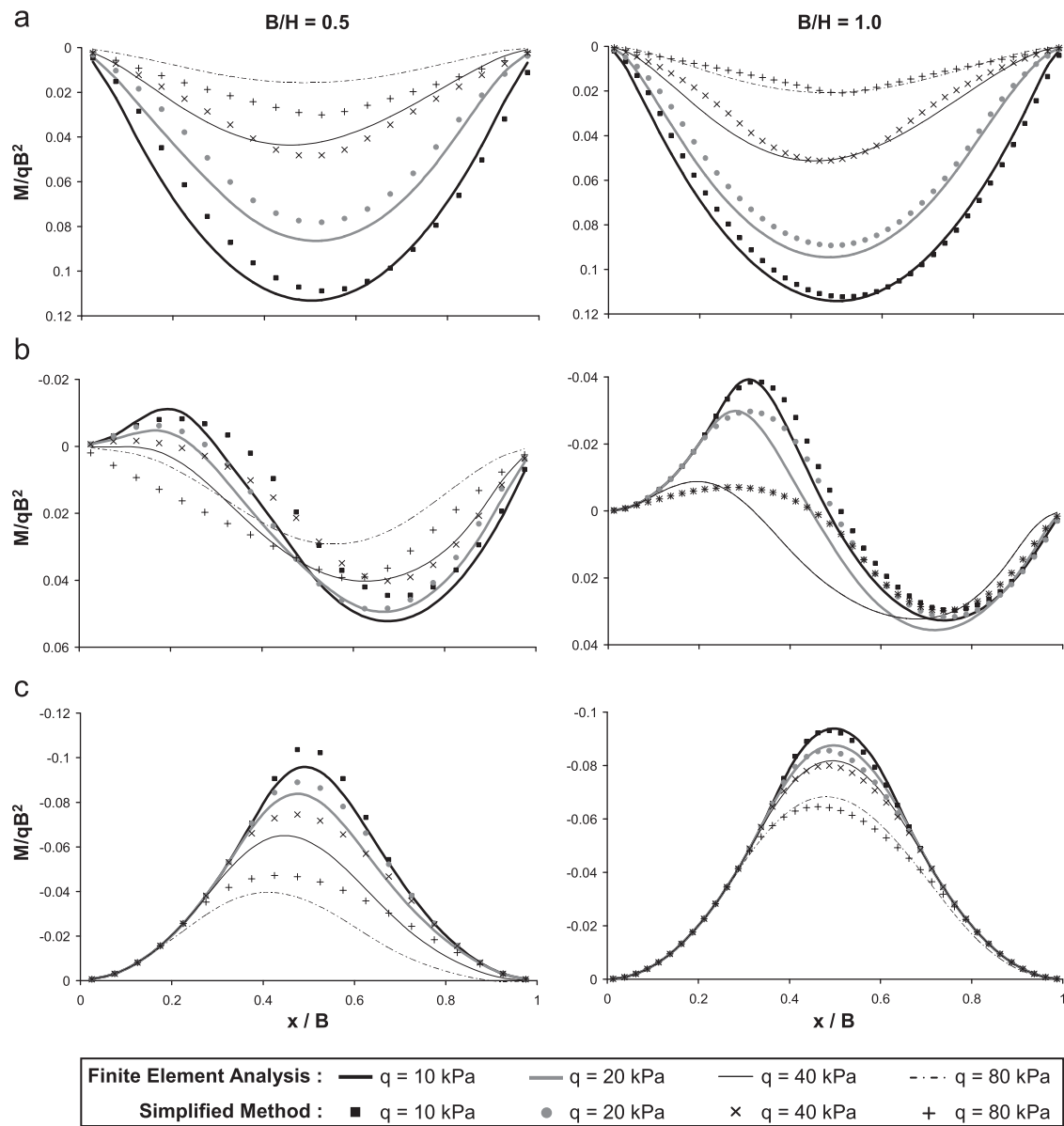


Fig. 14. Comparison of the simplified method with FE results for dense sand: normalised bending moment M/qB^2 for imposed bedrock offset $h/H=10\%$, for narrow $B/H=0.5$ and wide $B/H=1.0$ foundations: (a) $s/B=0.1$; (b) $s/B=0.5$ and (c) $s/B=0.9$.

analysis. The comparison is equally successful for the case of loose sand (not shown here due to space limitations).

As previously discussed, the stressing of the foundation (and consequently of the superstructure) depends largely on its position relative to the outcropping fault rupture. However, the exact location of a fault rupture at the ground surface can hardly be predicted, even if the location of the fault at bedrock is well known [1,9]. Hence, the design of a foundation–structure system has to be performed on the basis of design envelopes of internal forces, with respect to the location of the fault rupture s/B . Fig. 15 summarises the results of the comparison (between simplified method and FE results) for the M/qB^2 envelopes on dense and loose sand, for the case of the narrow $B/H=0.5$ foundation subjected to $h/H=10\%$ bedrock offset, and for three different normalised superstructure weights: $q/\rho gB=0.1$, 0.2, and 0.4. As expected, for light superstructure loads ($q/\rho gB=0.1$), where uplifting is prevalent, the comparison is excellent for both sand types. But even for heavier superstructure loads ($q/\rho gB=0.4$), and even on loose sand (i.e., cases in which the stressing is not related to detachment), the

simplified procedure provides reasonable, if slightly conservative, results.

4.3. Simplified design charts

The proposed simplified design procedure can be summarised in simplified design charts, such as those of Fig. 16 (referring to the narrow $B/H=0.5$ foundation subjected to $h/H=10\%$ bedrock offset). Such diagrams may provide, in normalised-terms, the effective foundation width (grey shaded areas) and the corresponding areas of equivalent loss of support (blank areas), as functions of: the surcharge load $q/\rho gB$, soil compliance (dense or loose soil), and the fault rupture location s/B . In all cases, the increase of $q/\rho gB$ leads to a suppression of the equivalent areas of loss of support (and, hence, reduction of foundation–structure distress). Soil compliance has a similar effect: b/B is larger in loose sand.

Fig. 17 illustrates schematically an example use of such simplified design charts (the example is shown for $B/H=0.5$,

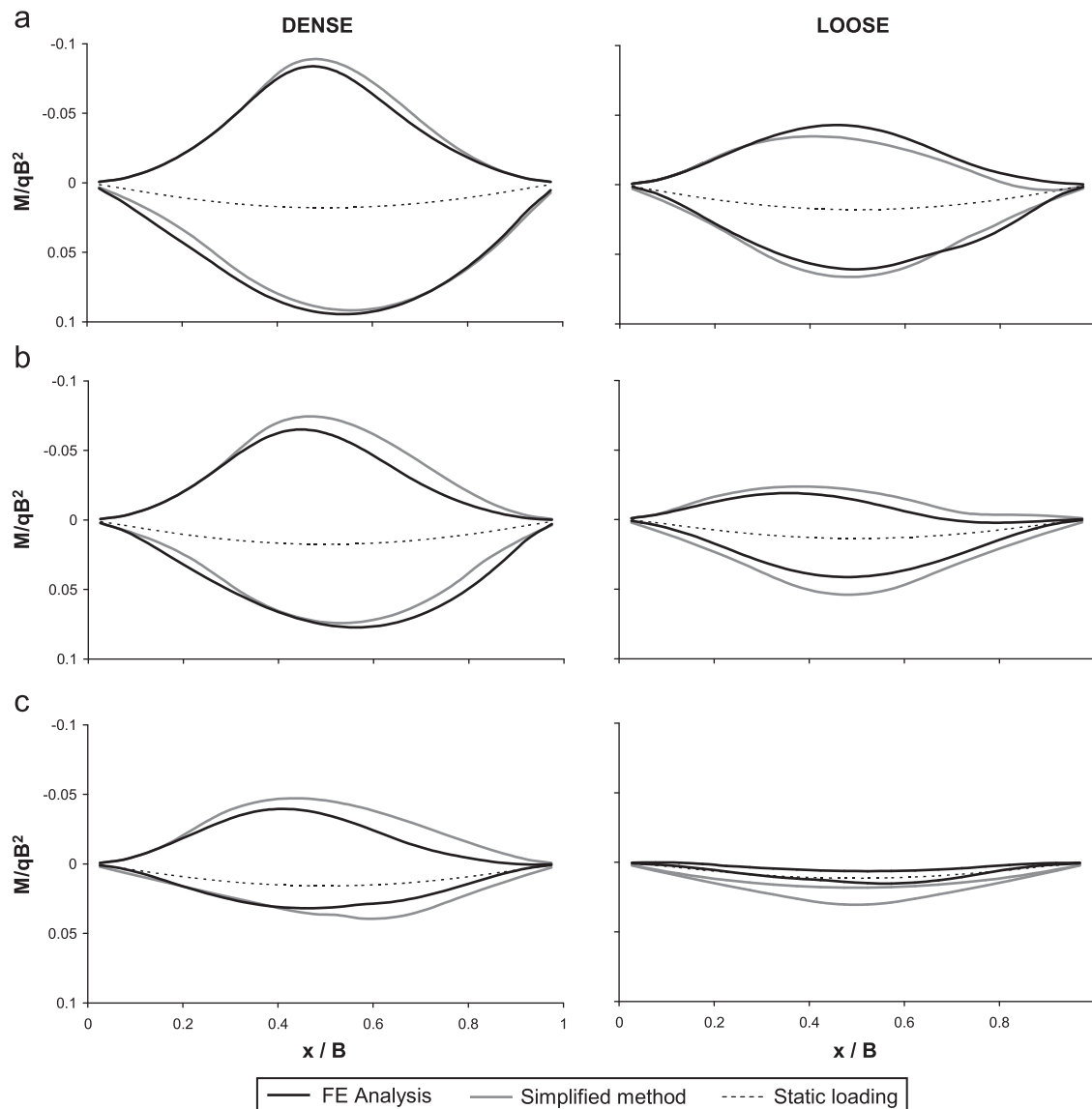


Fig. 15. Synopsis of analysis results: comparison of simplified method with FE analysis. Normalised bending moment M/qB^2 envelopes for dense and loose sand, for narrow $B/H=0.5$ foundation subjected to $h/H=10\%$ bedrock offset: (a) $q/\rho gB=0.1$, (b) $q/\rho gB=0.2$, and (c) (a) $q/\rho gB=0.4$.

$h/H=10\%$, dense sand, $s/B=0.1$). For example, if we would like to design a $B=10$ m structure with $q=20$ kPa (i.e., $q/\rho gB=0.1$) on a $H=20$ m dense sand deposit (i.e., $B/H=0.5$), subjected to $h=2$ m (i.e., $h/H=10\%$) thrust faulting at $s=1$ m (i.e., $s/B=0.1$), then according to the example design chart we would remove the support springs from the middle (Fig. 17a): $x/B=0.15$ – 0.84 (i.e., $x=1.5$ m– 8.4 m). If the same foundation was carrying a heavier superstructure load, $q=80$ kPa (i.e., $q/\rho gB=0.4$), then we would have to remove few support springs from under the left edge, $x/B=0$ to 0.04 , a few more from the middle, $x/B=0.52$ to 0.57 , and also from the right edge, $x/B=0.95$ to 1 (Fig. 17b). Naturally, the same procedure would have to be undertaken for all possible fault rupture locations ($s/B=0.3, 0.5, 0.7$, and 0.9), leading to different load combinations. Then, foundation and superstructure would be designed on the basis of the resulting internal force envelopes.

5. Summary, conclusions, and limitations

This paper applies a validated FE methodology to analyse the response of slab foundations subjected to thrust faulting.

Following a detailed parametric study, which aims at providing a deeper insight into the nature of fault rupture–soil–foundation interaction, a simplified design method is developed and validated against FE results. Example simplified non-dimensional design charts are presented for different foundation–structure systems and soil conditions. The main conclusions and limitations of this work are as follows:

- (1) The stressing of the foundation, and consequently of the superstructure, is a (rather-sensitive) function of its location relative to the fault outcrop. Depending on the geometry of fault crossing the structure, loss of support may take place either under the edges or under the middle of the foundation. In the first case, the unsupported spans act as cantilevers on a central “elastic” support, producing *hogging* deformation, while in the latter case as a simply supported beam on “elastic” end supports, producing *sagging* deformation.
- (2) The increase of the weight of the superstructure, expressed here in a simplified way through the surcharge load q , in general leads to less stressing of the foundation. The surcharge load has a double role: (i) it changes the stress

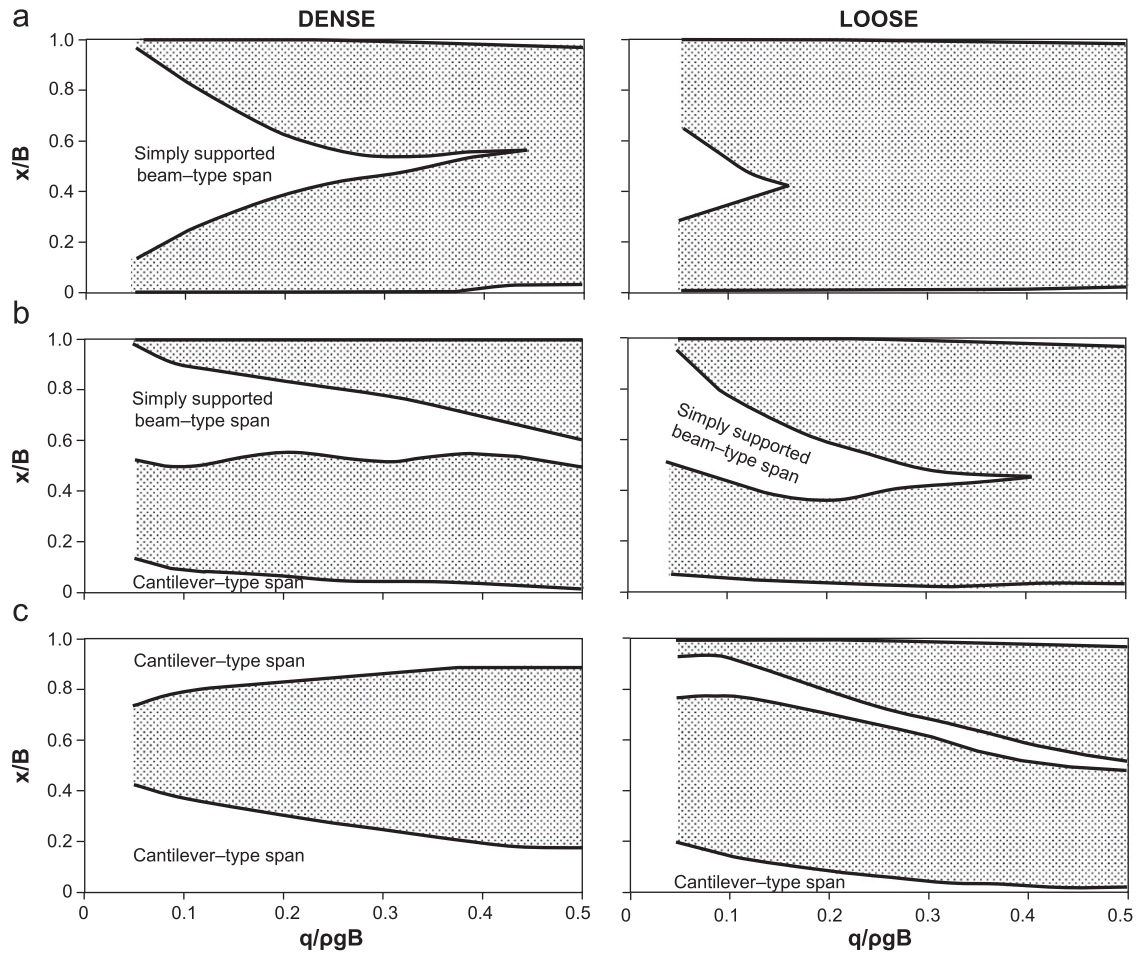


Fig. 16. Simplified design charts for “narrow” $B/H=0.5$ foundation subjected to $h/H=10\%$ bedrock offset: normalised effective foundation width (in grey) and corresponding equivalent areas of loss of support (in white), with respect to normalised surcharge load q/pgB and soil compliance. (a) $s/B=0.1$, (b) $s/B=0.5$ and (c) $s/B=0.9$.

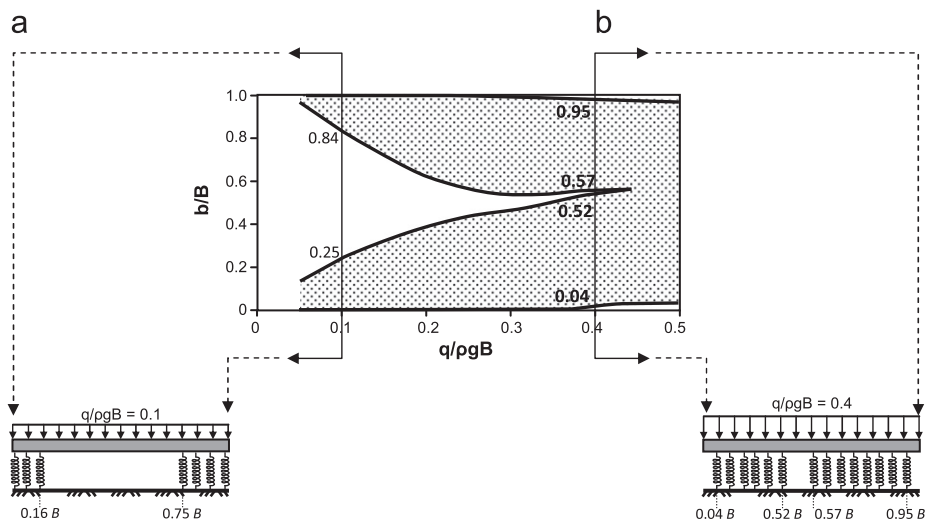


Fig. 17. Illustrative example of the use of the simplified design charts for two different structural loads. $B/H=0.5$ foundation, $h/H=10\%$, dense sand, $s/B=0.1$: (a) $q/pgB=0.1$ and (b) $q/pgB=0.4$.

field underneath the foundation, facilitating the diversion of the fault rupture; and (ii) by compressing the soil, it tends to “flatten” the faulting-induced anomalies of the ground surface.

(3) In all cases examined, soil density-and-stiffness is an important parameter controlling the stressing of the foundation. Founda-

tion-structure systems on loose silty sand will be subjected to less sagging or hogging deformation (depending on the location of fault crossing), and will thus experience far less stressing compared to a system on dense sand. In addition, increasing soil compliance leads to increased diffusion of plastic deformation underneath the foundation, facilitating

the aforementioned flattening of the faulting-induced anomalies (which are largely responsible for the distress).

- (4) Even when the fault rupture emerges beyond the structure, completely avoiding the foundation (by a distance of the order of at least one foundation width), the foundation slab may still experience substantial distress, with a sign reversal of the bending moments from their initial static values.
- (5) The stressing of the foundation stems mainly from loss of support. Exploiting the results of the parametric FE analysis, a simplified design procedure is developed for the design of foundation–structure systems against faulting. The concept is quite simple: remove the Winkler-type support springs from the area(s) of loss of support and conduct a conventional static analysis with the dead load q of the superstructure. But given that soil detachment is *not* always prevalent (as is the case with a light superstructure on dense soil) and that even a smaller reduction in soil reactions will have a deleterious effect on the developing bending moments, we define “equivalent” area(s) of loss of support. To this end, we utilise the negative areas in the $(p - q)/q$ vs. x/B diagram.
- (6) The simplified design procedure has been applied to all cases investigated herein. Simplified beam-on-Winkler spring analyses were conducted, removing the spring supports from the area(s) of equivalent loss of support. The comparison of the simplified procedure with FE results is shown to be satisfactory. The use of the method can be facilitated by a number of simplified design charts. The proposed simplified method should not be viewed as a general design tool, but as a first idea for a practical solution to the investigated problem.
- (7) Since the stressing of the foundation depends largely on its location relative to the emerging fault rupture, the design of a foundation–structure system must always be performed on the basis of design envelopes of internal forces, obtained from parametric variation of s/B .
- (8) The results presented in the paper refer only to idealised cohesionless soil deposits; they do not cover the whole range of soil profiles. Variations in foundation and superstructure stiffness (the rule, rather than the exception, in practice) should also be duly taken into account. All the presented results correspond to dry soil conditions. The effect of the presence of water has not been investigated. And finally, reverse faults at a dip angle of less than 60° exist, in fact abound, in nature; their effects however have not been explored in this paper.

Acknowledgement

The work of this chapter was conducted for the “DARE” project, which was financially supported by a European Research Council (ERC) Advanced Grant under the “Ideas” Programme in Support of Frontier Research (Grant Agreement 228254).

References

- [1] Anastasopoulos I, Gazetas G. Foundation–structure systems over a rupturing normal fault: Part I. Observations after the Kocaeli 1999 earthquake. *Bulletin of Earthquake Engineering* 2007;5(3):253–75.
- [2] Anastasopoulos I, Gazetas G. Behaviour of structure–foundation Systems over a rupturing normal fault: Part II. Analysis of the Kocaeli case histories. *Bulletin of Earthquake Engineering* 2007;5(3):277–301.
- [3] Anastasopoulos I, Gazetas G, Bransby MF, Davies MCR, El Nahas A. Fault rupture propagation through sand: finite element analysis and validation through centrifuge experiments. *Journal of Geotechnical and Geoenvironmental Engineering, ASCE* 2007;133(8):943–58.
- [4] Anastasopoulos I, Callerio A, Bransby MF, Davies MCR, El Nahas A, Faccioli E, Gazetas G, Masella A, Paolucci R, Pecker A, Rossignol E. Numerical analyses of fault–foundation interaction. *Bulletin of Earthquake Engineering* 2008;6(4):645–75.
- [5] Anastasopoulos I, Gazetas G, Bransby MF, Davies MCR, El Nahas A. Normal fault rupture interaction with strip foundations. *Journal of Geotechnical and Geoenvironmental Engineering, ASCE* 2009;135(3):359–70.
- [6] Berill JB. Two-dimensional analysis of the effect of fault rupture on buildings with shallow foundations. *Soil Dynamics and Earthquake Engineering* 1983;2(3):156–60.
- [7] Bransby MF, Davies MCR, El Nahas A. Centrifuge modelling of normal fault–foundation interaction. *Bulletin of Earthquake Engineering* 2007;6(4):585–605.
- [8] Bransby MF, Davies MCR, El Nahas A. Centrifuge modelling of reverse fault–foundation interaction. *Bulletin of Earthquake Engineering* 2007;6(4):607–28.
- [9] Bray JD. The effects of tectonic movements on stresses and deformations in earth embankments. University of California, Berkeley: PhD. Dissertation; 1990.
- [10] Bray JD. Developing mitigation measures for the hazards associated with earthquake surface fault rupture. *Workshop on seismic fault-induced failures—possible remedies for damage to urban facilities*. University of Tokyo Press; 2001. pp. 55–79.
- [11] Bray JD, Seed RB, Cluff LS, Seed HB. Earthquake fault rupture propagation through soil. *Journal of Geotechnical Engineering, ASCE* 1994;120(3):543–61.
- [12] Bray JD, Seed RB, Seed HB. Analysis of earthquake fault rupture propagation through cohesive soil. *Journal of Geotechnical Engineering, ASCE* 1994;120(3):562–80.
- [13] Brune JN, Allen CR. A low-stress-drop, low magnitude earthquake with surface faulting. The Imperial, California, Earthquake of March 4, 1966. *Bulletin of the Seismological Society of America* 1967;57:501–14.
- [14] Cole Jr DA, Lade PV. Influence zones in alluvium over dip-slip faults. *Journal of Geotechnical Engineering, ASCE* 1984;110(5):599–615.
- [15] Duncan JM, Lefebvre G. Earth pressure on structures due to fault movement. *Journal of Soil Mechanics and Foundation Engineering, ASCE* 1973;99:1153–63.
- [16] Erdik M. Report on 1999 Kocaeli and Düzce (Turkey) Earthquakes, in *Structural Control for Civil and Infrastructure Engineering*, 2001, Ed. by, F. Casciati, G. Magonette, World Scientific.
- [17] Eurocode EC8 structures in seismic regions. Part 5: foundations, retaining structures, and geotechnical aspects. Brussels: Commission of the European Communities; 1994.
- [18] Faccioli E, Anastasopoulos I, Callerio A, Gazetas G. Case histories of fault–foundation interaction. *Bulletin of Earthquake Engineering* 2008;6(4):557–83.
- [19] Gazetas G, Anastasopoulos I, Apostolou M. Shallow and deep foundations under fault rupture on strong seismic shaking. In: Pitilakis K, editor. *Earthquake geotechnical engineering*. Springer, 2007. p. 185–218 [Chapter 9].
- [20] Kelson KI, Kang K-H, Page WD, Lee C-T, Cluff LS. Representative styles of deformation along the Chelungpu fault from the 1999 Chi-Chi (Taiwan) Earthquake: geomorphic characteristics and responses of man-made structures. *Bulletin of the Seismological Society of America* 2001;91(5):930–52.
- [21] Leonidou EA, and Athanasopoulos GA. Bedrock fault rupture propagation in overlying cohesive soils: analysis with the FEM. *Proceedings of Greek National Conference on Geotechnical and Geoenvironmental Engineering* 2001; 2: 201–8.
- [22] Muir Wood D. *Geotechnical Modelling*. Spon Press: London.
- [23] Niccum MR, Cluff LS, Chamorro F, Wylie L. Banco Central de Nicaragua: A case history of a high-rise building that survived surface fault rupture. In: Humphrey CB, editor. *Engineering geology and soils engineering symposium*, Vol. 14. Idaho Department of Transportation; 1976. p. 133–44.
- [24] Palmer AC. *Dimensional analysis and intelligent experimentation*. Singapore: World Scientific Publishing; 2008.
- [25] Pamuk A, Kalkan E, Ling HI. Structural and geotechnical impacts of surface rupture on highway structures during recent earthquakes in Turkey. *Soil Dynamics and Earthquake Engineering* 2005;25:581–9.
- [26] Roth WH, Scott RF, Austin I. Centrifuge modelling of fault propagation through alluvial soils. *Geophysical Research Letters* 1981;8(6):561–4.
- [27] Stone KJL, Muir Wood D. Effects of dilatancy and particle size observed in model tests on sand. *Soils and Foundations* 1992;32(4):43–57.
- [28] Taylor CL, Cline KM, Page WD, Schwartz DP. The Borah Peak, Idaho Earthquake of October 28, 1983—surface faulting and other phenomena. *Earthquake Spectra* 1985;2(1):23–49.
- [29] Ulusay R, Aydan O, Hamada M. The behaviour of structures built on active fault zones: examples from the recent earthquakes of Turkey. *Structural Engineering & Earthquake Engineering, JSCE* 2002;19(2):149–67.
- [30] Yould TL, Bardet J-P, Bray JD. Kocaeli, Turkey, Earthquake of August 17, 1999 Reconnaissance Report. *Earthquake Spectra* 2000;16(Suppl. A):456.
- [31] Wang L. The characteristics of disasters induced by the Wenchuan M_w 8.0 Earthquake. In: Prakash S, editor. *China 2008, International conference on case histories in geotechnical engineering*. Washington, DC, 2008.